Probing molecular structures at buried solid/solid interfaces involving low-*k* materials or polymers *in situ* nondestructively: a review

Shuqing Zhang,[a,b] **Guangyao Wu**,[a] **and Zhan Chen**[a,b,*]
[a]University of Michigan, Department of Chemistry, Ann Arbor, Michigan, United States
[b]University of Michigan, Department of Macromolecular Science and Engineering, Ann Arbor, Michigan, United States

Abstract

Background: With the development of three-dimensional (3D) integration technology including extreme ultraviolet (EUV) lithography, more and more buried interfaces are involved in a device. It is important to probe such buried solid/solid interfaces *in situ*, but due to the lack of appropriate metrology, it is difficult to do so.

Aim: This review aims to introduce sum frequency generation (SFG) vibrational spectroscopy to researchers and engineers in the research fields related to 3D integration technology including EUV lithography. SFG can probe buried solid/solid interfaces in situ nondestructively.

Review Approach: This review presents the SFG technique and the recent results obtained from SFG studies on a variety of solid/solid interfaces, including porous low-*k* material/silicon interfaces, plasma treated polymer/epoxy interfaces, flux treated metal/epoxy interfaces, chemical reactions at buried solid/solid interfaces, and structures of buried solid/solid interfaces in multilayered thick device.

Conclusions: SFG has been successfully applied to elucidate molecular structures and molecular interactions at buried solid/solid interfaces *in situ* nondestructively. SFG has great potential to probe buried interfaces in devices based on 3D integration technology.

 [DOI: 10.1117/1.JMM.22.3.031202]

Keywords: buried interfaces; sum frequency generation vibrational spectroscopy; adhesion; low-*k* materials; flux; interfacial chemical reactions.

Paper 22070SSV received Nov. 11, 2022; accepted for publication Feb. 8, 2023; published online Mar. 2, 2023.

1 Introduction

In recent years, the continuous scaling of semiconductor technology has greatly benefitted from the rapid development of three-dimensional (3D) integration technology and 3D transistors.[1–7] It is expected that there will be an urgent need for further progress on more complicated 3D devices and 3D dynamic random-access memory (3D DRAM) in the future. During this process, it is necessary to develop and adopt many innovative metrologies to characterize 3D devices and 3D units to achieve an in-depth understanding of the structure-function relationships of new devices and new materials, aiding in the design of advanced 3D devices with improved performance. As the 3D devices become more and more complicated, more buried solid/solid interfaces are involved, while molecular interactions at such buried interfaces play key roles in determining the performance of the entire device and should be investigated *in situ*.

Extreme ultraviolet (EUV) lithography has been adopted for 3D technology, which has increasing numbers of passes, in high volume manufacturing of 7- and 5-nm node logic integrated circuits and 16/14-nm node DRAM.[8–10] Compared with 193-nm immersion lithography,

*Address all correspondence to Zhan Chen, zhanc@umich.edu

EUV lithography enhances resolution, reduces the number of lithographic passes for critical device levels, improves pattern fidelity and reduces manufacturing cost when adopted appropriately. Recently a new EUV resist technology was developed, where both the resist deposition and the resist development can be conducted in a dry gaseous phase. The performance of EUV dry resist depends on the intricate interactions between the EUV dry resist layer and the underlying layer beneath of the EUV dry resist, called underlayer. In addition, the top surface of the underlayer, even well-characterized *a priori*, undergoes possible chemical and physical modifications during the deposition of the EUV dry resist layer, which needs to be characterized *in situ* at the buried interface.

Technique to characterize the molecular structure and molecular interactions between the EUV dry resist layer and the underlayer at the buried interface *in situ* nondestructively is urgently needed, which could provide valuable information to optimize the underlayer structure and improve EUV resist technology. For many other buried interfaces involved in 3D technology, it is also necessary to probe buried interfaces *in situ* in real time.

It is difficult to probe molecular structures and molecular interactions at buried interfaces *in situ*, due to the lack of appropriate metrology. Typically, to probe a buried solid/solid interface, the interface was separated and two exposed surfaces were examined. This method is not a satisfactory approach because a buried interface with good adhesion cannot be easily broken. When the interface is separated, the original molecular interactions and molecular structure at the buried interface were likely altered, thus the results obtained from the investigations on the two exposed surfaces are different from those at the buried interface.

Sum frequency generation (SFG) vibrational spectroscopy,[11–37] a second-order nonlinear optical spectroscopy, has been developed into a powerful tool to study buried interfaces *in situ* in real time nondestructively.[12,13,38–41] The sub-monolayer surface/interface sensitivity is due to the intrinsic selection rule, which will be presented in more detail below. It is worth mentioning that SFG has not been extensively applied to study buried interfaces in 3D devices and buried interfaces involving EUV dry resist yet, but previous studies clearly demonstrated its feasibility, power, and uniqueness in studying buried solid/solid interfaces *in situ*. We are confident that SFG will be able to elucidate molecular interactions and molecular structures at buried interfaces involved in devices based on 3D technology including EUV lithography. In this paper, we will briefly review several examples of applying SFG to study buried solid/solid interfaces in our lab at the University of Michigan, demonstrating the potential and feasibility of developing SFG into important metrology for 3D integration technology.

2 Metrology: Sum Frequency Generation Vibrational Spectroscopy

SFG is a second-order nonlinear optical spectroscopic technique.[11–44] According to the selection rule of a second-order nonlinear optical process, SFG signal can only be generated from a medium with no inversion symmetry under the electric dipole approximation.[11–44] Most bulk materials possess inversion symmetry, therefore, no SFG signal can be produced. Surfaces and interfaces lack inversion symmetry, thus, they can produce SFG signals. Both experiments and theoretical calculations indicate that SFG is sub-monolayer surface/interface sensitive. In an SFG experiment, a visible laser and a frequency tunable infrared (IR) laser overlap on a surface/interface to generate a signal with a sum frequency of the two input beams (Fig. 1). The SFG signal intensity is detected while the IR input beam frequency is tuned. When the IR beam frequency matches a vibrational resonance of the surface/interface, the SFG signal intensity is enhanced. The SFG intensity is plotted versus the wavenumber of the input IR beam, producing a vibrational spectrum of the surface or interface. Vibrational spectra are fingerprints of molecules, thus SFG spectra can provide molecular interfacial structures such as the presence, coverage, orientation, and ordering of molecules at interfaces. Molecular interactions, such as chemical reactions, hydrogen bonding formation, and van der Walls interactions at buried interfaces can be revealed. SFG is an excellent technique which can be applied to study buried interfaces *in situ* nondestructively at the molecular level.

SFG is a spectroscopic technique. The beam sizes of the input beams on the samples are around 500 μm. In an SFG spectrum, we can deduce the surface/interfacial presence of various

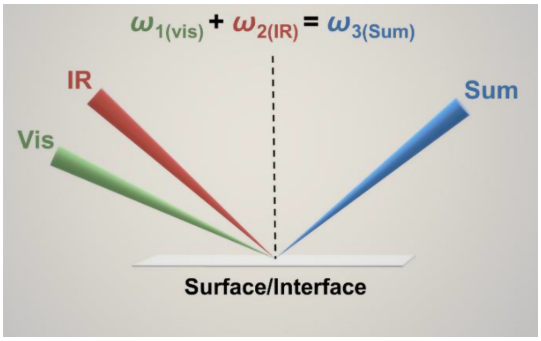

Fig. 1 SFG sample geometry. Two input beams overlap on the sample interface while the sum frequency signal is collected.

functional groups from the peak centers. The orientations of various surface/interfacial functional groups could be determined by the SFG spectra collected using different polarizations of the input and outgoing beams such as ssp (s-polarized SFG signal beam, s-polarized input visible beam, and p-polarized input IR beam), ppp, or sps. Usually, an SFG system contains a pico-second or femto-second laser, a nonlinear optical system with optical parametric generation/optical parametric application/different frequency generation stages, a sample stage, and a detection system. SFG has been extensively applied to study surfaces and interfaces, including buried solid/solid interfaces.[38,39,41–47] In the following, we will present several examples to demonstrate that SFG can probe buried solid/solid interfaces to elucidate molecular interactions and molecular structures of buried interfaces *in situ*.

3 Results and Discussion

3.1 *Buried Interfaces between Low-k Materials and Silicon Substrate*

SFG has been successfully applied to investigate the surface and buried interface of low-*k* thin film coating on silicon.[42–47] Low-*k* materials and copper have been introduced to replace silicon dioxide and aluminum as interconnections in high performance integrated circuits to improve resistance-capacitance delay, minimize crosstalk-noise, enhance signal transmission, and reduce power dissipation. Porous organosilicate (pSiCOH) materials have been extensively used as low-*k* interlayer dielectric materials.[48,49] Such materials are very porous, and may crack and delaminate during polishing and may be damaged due to the plasma/chemical treatment while being processed. Therefore, it is crucial to understand their surface changes and buried interfacial behavior.

We have studied surface/interfacial molecular structures of a thin film deposited on a substrate or sandwiched between two media.[43,50,51] When a film is thin, the SFG signals collected from the film have signal contributions from both sides (a surface and an interface, or two interfaces). Such signal contribution is related to the Fresnel coefficient of each surface or interface. By varying the thickness of the film, the Fresnel coefficient of each surface or interface changes. Therefore, using SFG spectra collected from the films with different thicknesses, we could deconvolute the signals from each surface or interface.[50,51] For certain cases (or particular thicknesses), the Fresnel coefficient of a surface or interface can be minimized. Thus, the SFG signals collected from the film are dominated by the contributions of other surface or interface.[43] Based on this method, we first developed a generally applicable way to elucidate molecular structures of the surfaces and buried interfaces of low-*k* films using SFG measurements, e.g., spin-coated poly(methylsilsesquioxane) (PMSQ) films of different thicknesses [Fig. 2(a)].[43] SFG ssp and ppp spectra were collected from these thin low-*k* samples, which were contributed by both the PMSQ/air and buried PMSQ/silicon interfaces [Figs. 2(b) and 2(c)]. Through detailed data analysis, we found that the ssp spectra were dominated by the contributions from the PMSQ/air interface, while the ppp spectra were contributed by both the PMSQ/air and buried PMSQ/silicon interfaces. From the ssp spectra, the PMSQ/air structure could be deduced,

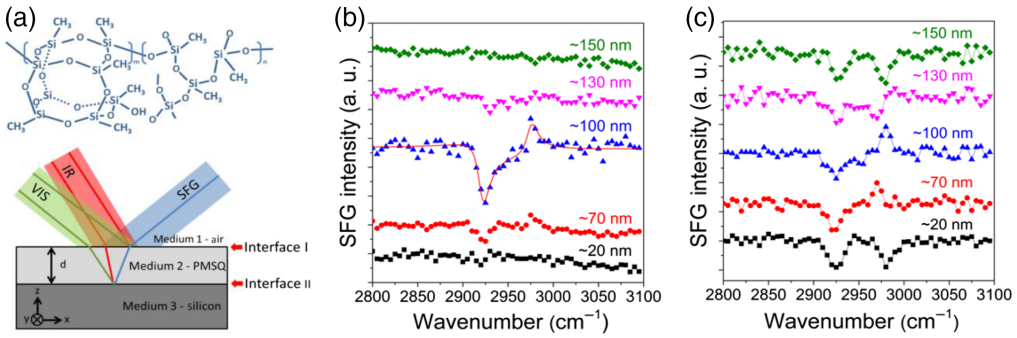

Fig. 2 (a) Molecular structure of the low-*k* material PMSQ used in this study. Bottom: SFG experimental geometry used to collect SFG spectra from the low-*k* film on silicon. Two input beams overlap on the sample interface while the sum frequency signal is collected. SFG (b) SSP and (c) PPP spectra collected from PMSQ films of different thicknesses on silicon substrates. (b) The solid red curve is the fitting result. (c) The solid curves connecting the data points are a guide to the eye. Adapted with permission from Ref. 43. Copyright 2015, American Chemical Society.

which could be used to calculate the PMSQ/air surface contribution to the ppp spectra. After deconvoluting such PMSQ surface contribution from the collected ppp spectra, the ppp signal contributed from the buried interface could be deduced (Fig. 3), from which the structure of the buried PMSQ/silicon interface could be determined.[43]

The two SFG vibrational peaks in Fig. 2 at ~2920 and ~2975 cm^{-1} were contributed by the symmetric and asymmetric C—H stretching of the Si-CH_3 groups, respectively. From the above data analysis, it was found that the methyl groups oriented at 37 and 75 deg versus the surface normal at the PMSQ/air and buried PMSQ/silicon interfaces.

This generally applicable data analysis method was successfully applied to study the plasma treatment effect on low-*k* pSiCOH coatings with different porosities, using methyl group orientation and coverage as indicators to demonstrate the plasma treatment effect.[45] The low-*k* coatings studied in this project were prepared by PECVD with 7% and 25% porosities respectively. SFG ssp and ppp spectra were collected from the two samples before and after 5-s oxygen plasma exposure. Using the developed data analysis methodology, it was determined that for the pSiCOH sample with 7% porosity, the methyl group on the surface in air before and after plasma treatment oriented at 48 and 41 deg versus the surface normal respectively, while the surface coverage of methyl was only 36% remained after the plasma treatment. This shows that the 5s-plasma treatment could substantially change the pSiCOH surface structure. Interestingly, the methyl coverage and orientation (~80 deg) at the buried pSiCOH/silicon interface before and after the plasma treatment remained the same, indicating that the plasma treatment did not alter the buried SiCOH interfacial structure on silicon.[45]

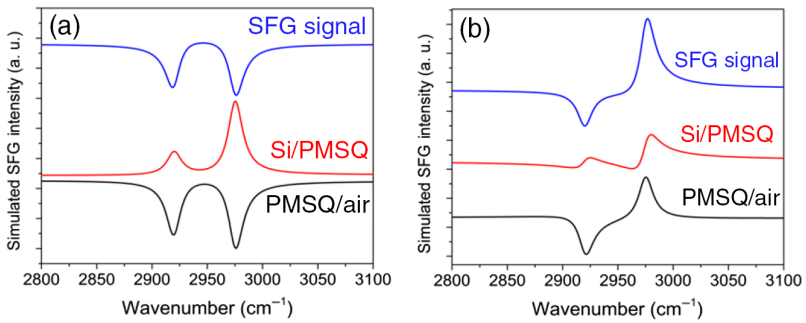

Fig. 3 Simulated SFG ssp spectra of (a) 20- and (b) 100-nm thick PMSQ films and deduced contributions to the simulated SFG spectra from the surface and buried interface signal. Adapted with permission from Ref. 43. Copyright 2015, American Chemical Society.

For a more porous pSiCOH film with 25% porosity, before the plasma treatment, the methyl group on the surface in air oriented at 38 deg versus the surface normal. After the plasma treatment, the orientation angle was determined to be 55 deg with a different absolute orientation, changing from a pointing up (to air) to a pointing down (to SiCOH film bulk) absolute orientation. The methyl surface coverage was 60% after the plasma treatment. We believe that the detected absolute orientation change was caused by the etching effect: After the plasma treatment, a new layer of methyl groups was exposed to air on the surface. The methyl group orientation (~80 deg) and coverage at the buried SiCOH/silicon interface remained the same after the plasma treatment, showing that even with a high (25%) porosity, plasma treatment did not damage the buried SiCOH/silicon interface of the low-k SiCOH film.[45]

Similar SFG experiments and data analysis methods were used to study PECVD prepared pSiCOH film after NH_3 plasma treatment as well as surface repair by silylation under UV irradiation.[46] It was found that the pSiCOH surface could be substantially damaged by NH_3 plasma treatment, while the repair method used in this study could effectively repair the surface structures but will not recover completely the entire plasma-damaged layer. The buried pSiCOH/silicon interface was not influenced by either the NH_3 plasma treatment or the silylation repair.[46] Similarly, molecular structures at the surface and buried interface of a low-k pSiCOH were examined before and after reactive ion etching (RIE) and subsequent dielectric repair using SFG. It was also found that RIE treatment and repair did not alter the buried pSiCOH interface.[47]

3.2 *Effect of Polymer Surface Plasma Treatment on Buried Polymer/Epoxy Interfaces*

Strong adhesion is required for many interfaces in microelectronics. For example, poor adhesion at the polyimide (PI) and epoxy interface in flip-chip packages can lead to the propagation of cracks, moisture diffusion, and corrosion of solder bumps (metallic interconnections).[52–54] Plasma treatment on polymer surfaces is an important process to enhance the adhesion between the polymers and various materials. SFG has been applied to study molecular structural changes of polymer surfaces after plasma treatment and their impact on buried interfaces.[35,55] Such studies provide molecular-level understanding of important polymer adhesion in microelectronics.

SFG was applied to study the surface structures of covered polymer materials after plasma treatment [Fig. 4(a)] to simulate the plasma treatment in industrial processes.[55] It was found that with a cover, plasma treatment has varied impacts on different positions [Fig. 4(b)] of the polymer surface. Figures 4(c) and 4(d) show that the SFG spectra collected from the edge and center positions of a polystyrene (PS) surface were similar, dominated by the aromatic C–H stretching signals. After a 10-s air plasma treatment, the SFG signals collected from the edge positions on the PS surface exhibited substantial changes, with greatly reduced SFG signal intensity, while no noticeable surface change was observed from the center of the polymer surface. This is because it would take more than 10 s for plasma to reach the sample center with the cover.

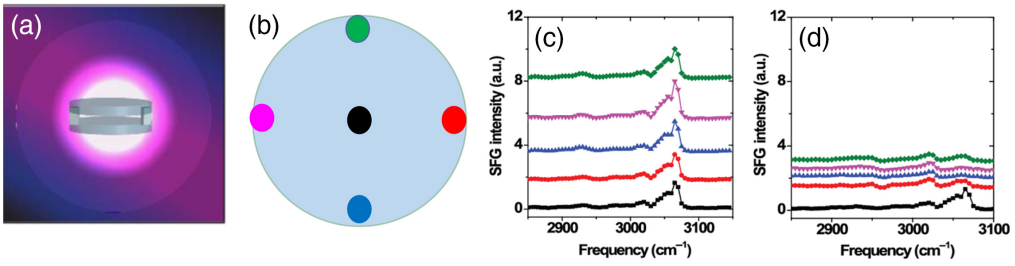

Fig. 4 Schematics showing (a) sandwich of the sample and protective cover in plasma chamber and (b) sample positions probed by SFG. (c) and (d) SFG spectra collected from the center and edge positions before (c) and after (d) air plasma, respectively. The black, red, blue, pink, and green spectra were collected from the center, 3 o'clock, 6 o'clock, 9 o'clock, and 12 o'clock positions, respectively. Adapted from Ref. 55. Copyright 2017, IEEE.

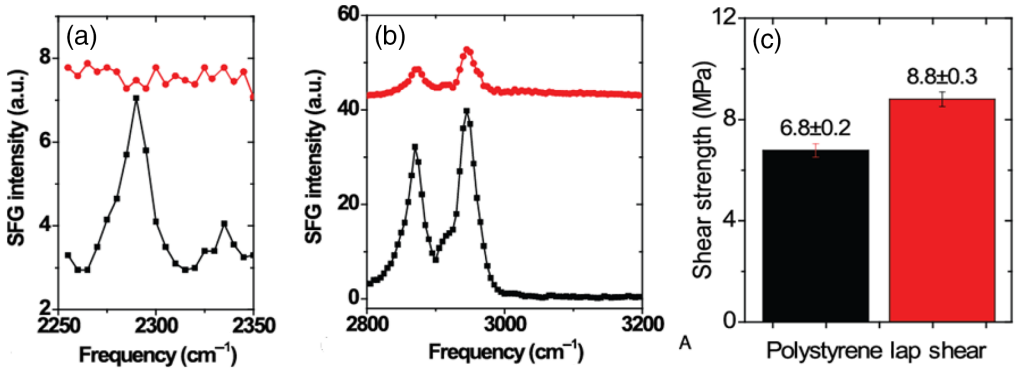

Fig. 5 (a) SFG ssp spectra of the dPS (before plasma treatment)/epoxy buried interface (black) and the dPS (after plasma treatment)/epoxy interface (red) in the C-D stretching frequency region. (b) SFG ssp spectra of the dPS/epoxy buried interface before (black) and after (red) 100 s He plasma treatment on dPS surface. (c) Adhesion strengths measured from the PS (before plasma treatment)/epoxy interface (black) and the PS (after plasma treatment)/epoxy interface (red) with the lap shear tests. Adapted from Ref. 35. Copyright 2017, Royal Society of Chemistry.

The detailed SFG data analysis showed that after the plasma treatment on the PS surface, the phenyl surface density decreased and the surface phenyl groups changed orientation to lie down more onto the PS surface with a broader orientation distribution.[55] The results obtained from our model study could be correlated to the observations in manufacture. In the plasma treatment process in industry, a large plasma treatment chamber was used, with a magazine rack for holding trays and all samples for treatment. Some samples may not be able to be exposed to plasma with the short treatment time, leading to later adhesion failure.

In addition to the PS surface, plasma treatment on the covered PI surface was also investigated using SFG. Similarly, it was found that the plasma treatment changed the structure on the surface edge more substantially than the center position on the surface. The PI imide ring lies down more on the surface after the plasma treatment.[55]

We then applied SFG to study buried interfaces between plasma treated PS or PI and epoxy to understand the effect of polymer surface plasma treatment on buried interfacial structure.[35] Here to avoid spectral confusion, deuterated PS (dPS) was used in the study. SFG results show that after a 100-s He plasma treatment, the dPS surface was totally disordered, generating no SFG signal. SFG spectra collected from the buried dPS/epoxy interface [Figs. 5(a) and 5(b)] show that at the buried interface, dPS was still disordered, and the ordering and coverage of interfacial methyl groups from epoxy greatly decreased.[35] As we reported previously in the literature, for epoxy materials, less interfacial methyl groups lead to stronger adhesion.[56] Therefore the adhesion between the plasma treated dPS and epoxy was measured to be higher [Fig. 5(c)]. Similar results could be obtained from plasma treated PI.[35] SFG results indicated that the disordering of the PI at the buried PI/epoxy interface (caused by the plasma treatment on PI) induced fewer methyl groups at the interface, leading to higher adhesion.[35]

Epoxy has been widely used as adhesive for a variety of applications in the microelectronics industry. It is worth mentioning that we have extensively applied SFG to study the interfacial behavior of model and commercial epoxy materials at buried interfaces. SFG results demonstrated that interfacial diffusion plays a significant role in enhancing epoxy adhesion, while methyl groups in epoxy formulation could reduce adhesion by segregating at the interface with ordering.[56] Addition of a small number of silane molecules (e.g., 2 wt%) to epoxy could improve the adhesion strength of epoxy, and minimize the adhesion loss after hydrothermal treatment.[57,58]

3.3 *Molecular Behavior of Flux Molecules at Buried Interfaces*

As discussed above, epoxy materials are widely used in microelectronic devices. Adhesion of epoxies to many types of substrates (composite materials, metals, and polymers), along with different types of surface treatments, is encountered. Electronic chips or dies are typically attached to lead frames through copper posts. The flux material is commonly used to treat copper

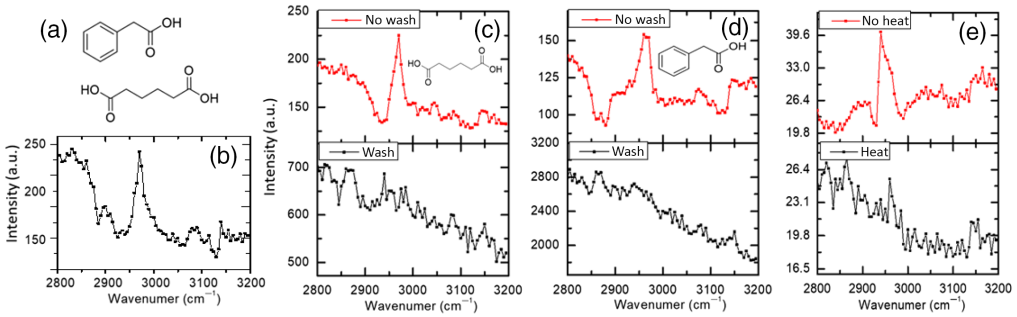

Fig. 6 (a) Molecular structures of phenylacetic acid (top) and adipic acid (bottom). (b) SFG ppp spectrum from the copper (without flux treatment)/epoxy buried interface. (c)–(e) SFG ppp spectra collected from copper (with flux treatment without washing or heating)/epoxy interface (top) and copper (with flux treatment with washing or heating)/epoxy interface (bottom). Samples studied in (c)–(e) were treated by adipic acid, phenylacetic acid, and commercial flux respectively. Adapted from Ref. 61. Copyright 2021, ASME.

surfaces allowing better wettability and electrical contact. However, flux residues could be left behind on exposed surfaces, causing voids in epoxy underfills and poor epoxy adhesion to die and substrate, reducing the device's performance. Therefore, it is important to investigate flux residue interfacial behavior and related interfacial effects. Typically, the flux material used in industry is a proprietary blend of water, organic compounds, salts, and carboxylic acids or amines.[59,60] We applied SFG to study the interfacial molecular behavior of flux molecules using model fluxes as well as a commercial flux sample.[34,61]

Figure 6(a) shows the molecular structures of the two model flux molecules phenylacetic acid and adipic acid. The SFG spectra collected from these two molecules on copper are very different.[61] Interestingly, SFG spectra collected from the epoxy/copper interfaces with copper flux treated with these two molecules are very similar, and similar to that collected from the epoxy/copper interface without the treatment of flux molecules on copper [Figs. 6(b)–6(d)]. Therefore the interfaces between epoxy and flux treated copper are dominated by ordered epoxy molecules. With washing the flux on copper, SFG signals collected from the copper (flux treated and then washed by water)/epoxy interface only show nonresonant signals from copper [Figs. 6(c) and 6(d)], indicating disordered interfaces.

In addition to the model flux molecules, we also investigated a commercial flux, Kester 979 no-rinse flux, which requires no washing to clean—it can be cleaned by heating. SFG spectrum collected from the buried interface between epoxy and commercial flux treated copper is shown in Fig. 6(e). This spectrum is similar to those collected from the interfaces between epoxy and copper treated by the two model fluxes, as well as that detected from the interface between epoxy and copper without flux treatment. This again shows that at the buried interface between epoxy and commercial flux treated copper, epoxy molecules dominated the interface. After heating, the SFG spectrum collected from the epoxy/copper (treated by commercial flux and heated) interface also only shows the SFG nonresonant signals from copper, as the model flux cases after washing the flux with water presented above, indicating a disordered interface.

Figure 7 shows the adhesion testing results of various interfaces. The adhesion strengths measured at the interfaces between epoxy and copper with model or commercial flux treated without washing or heating were found to be similar, and also similar to that measured at the interface between epoxy and copper without any flux treatment. This agrees with the above SFG results which showed that these interfaces were similar with dominated epoxy at the interface. The adhesion strengths greatly increased after washing or heating the copper after flux treatment to remove the flux from copper to clean the copper surface (Fig. 7). The adhesion increase is due to the disordered interface between epoxy and copper surface after flux treated the copper surface by removing the surface oxide layer (confirmed by grazing incidence x-ray diffraction experiments).[61]

This study demonstrated that SFG is a powerful tool to study flux behavior at buried solid/solid interfaces *in situ* nondestructively. SFG was not only able to study the interfacial behavior of model flux compounds, but also successfully investigated commercial flux at the interface.

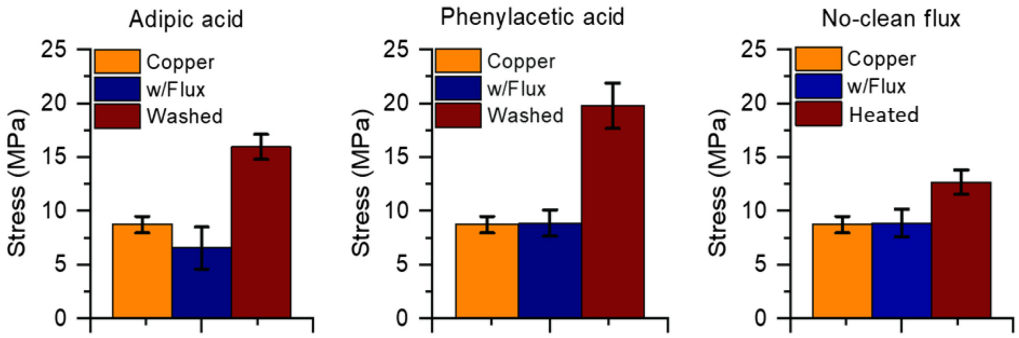

Fig. 7 Lap shear adhesion test data from adipic and phenylacetic acid model fluxes, and the no-clean commercial flux. Copper is the control with no flux added to copper, w/Flux are samples with flux at the buried interface, and "wash" or "heated" is with the flux cleaned by washing or heating before preparing the buried interface. Adapted from Ref. 61. Copyright 2021, ASME.

3.4 *Chemical Reactions at Buried Interfaces*

Chemical reactions forming covalent bonds at buried interfaces could greatly enhance the interfacial adhesion, which have been widely used in many applications. However, the detailed mechanisms of such interfacial chemical reactions remain unknown because it is difficult to probe chemical reactions at buried solid/solid interfaces *in situ* in real time. In recent years, we have applied SFG to study chemical reactions at a variety of buried solid/solid interfaces, especially buried interfaces involving polymers.[30,62–65] Here, we want to present two examples.

SFG has been applied to study the adhesion mechanisms of nylon and modified polyethylene.[62] A small amount of maleic anhydride (MAH) groups were grafted to poly(ethylene-octene) (MAHgEO), which could greatly enhance the adhesion to nylon. SFG was applied to study the buried interface between nylon and MAHgEO. It was found that the N–H stretching signals which could be detected from the nylon surface [Fig. 8(a)], disappeared at the nylon/MAHgEO interface [Fig. 8(b)], due to the chemical reactions between MAH groups and nylon at the buried interface. Without MAH grafted, SFG signals could be collected from the nylon/EO interface [Fig. 8(c)]. Nylon has NH_2 end groups and NH groups in the backbone. To understand whether NH_2 or NH or both participated in the interfacial reactions, SFG spectra were also collected from the C═O stretching frequency region [Figs. 8(d)–8(f)], showing that the nylon C═O groups participated in the interfacial reaction, thus it is believed that nylon NH group was also involved in the interfacial chemical reaction. The reaction mechanisms can be deduced from the SFG studies, as shown in Fig. 9.

Time-dependent and temperature-dependent SFG studies were also performed on the buried nylon/MAHgEO interfaces. The activation energy of the chemical reaction between nylon and MAHgEO was determined to be 33 kJ/mol at the interface, not very different from the value of

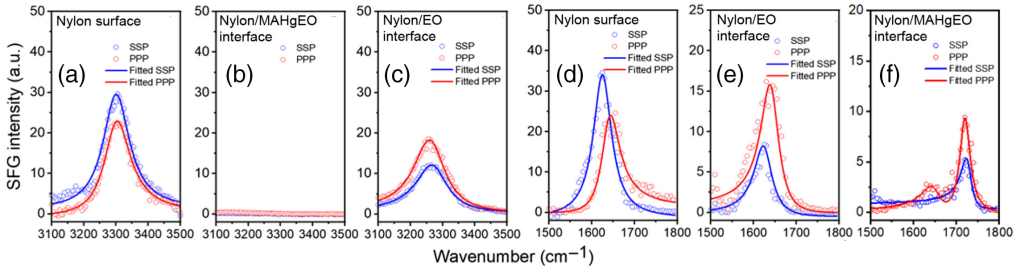

Fig. 8 SFG ssp and ppp spectra collected in the amine N-H stretching frequency region from: (a) a nylon-air surface; (b) nylon/MAHgEO interface after reaction; and (c) nylon/EO interface. SFG ssp and ppp spectra collected in the carbonyl C═O stretching frequency region from (d) nylon-air surface; (e) buried nylon/EO interface; and (f) buried nylon/MAHgEO interface. The open circles and solid lines are experimental data and fitting curves, respectively. Adapted from Ref. 62. Copyright 2020, American Chemical Society.

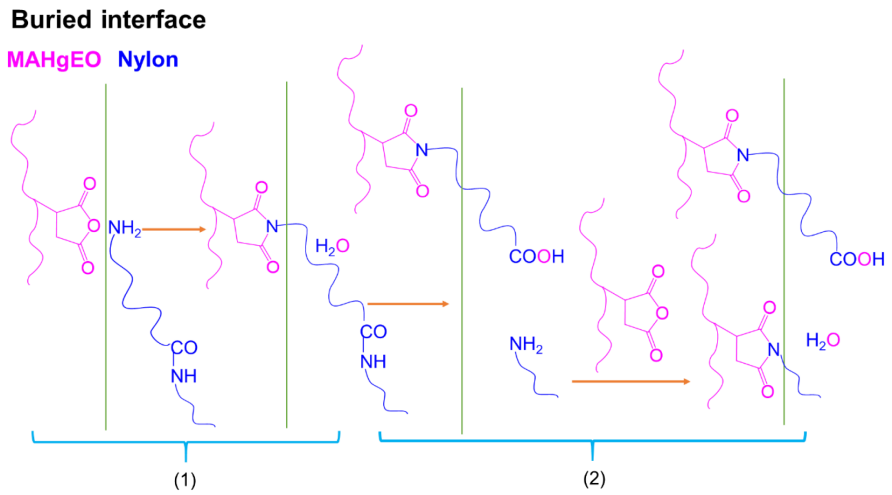

Fig. 9 Two reaction mechanisms [(1) and (2)] at a buried nylon/MAHgEO interface that result in the formation of imide and carboxylic acid. Adapted from Ref. 62. Copyright 2020, American Chemical Society.

the bulk reaction (53 kJ/mol). To the best of our knowledge, this is the first direct detection and quantification of a chemical reaction (the consumption of reactants and the formation of products simultaneously) between two polymers at the buried solid/solid interface. Using a similar approach, we also studied interfacial chemical reactions between EVOH and MAHgEO.[63]

Isocyanate-based primers are extensively used for many different substrates to enhance the adhesion to sealants or potting compounds, e.g., polyurethane potting compound (PPC). We have applied SFG to study the molecular interactions at the buried primer/PPC interface to understand the molecular mechanisms of adhesion between primer and PPC.[64] SFG spectra were collected from the primer/PPC interface before and after annealing, as shown in Figs. 10(a) and 10(b). Before annealing, a strong SFG peak centered around 2250 cm^{-1} was observed, contributed by the isocyanate −N═C═O stretching mode from the primer at the interface. After annealing, this signal disappeared due to the interfacial chemical reaction. Figures 10(c) and 10(d) present SFG spectra collected in a different frequency region, showing that after annealing, a urea C═O stretching signal was detected from the reaction product of the primer-PCC reaction at the buried interface. This urea signal was not detected from either primer or PCC without the

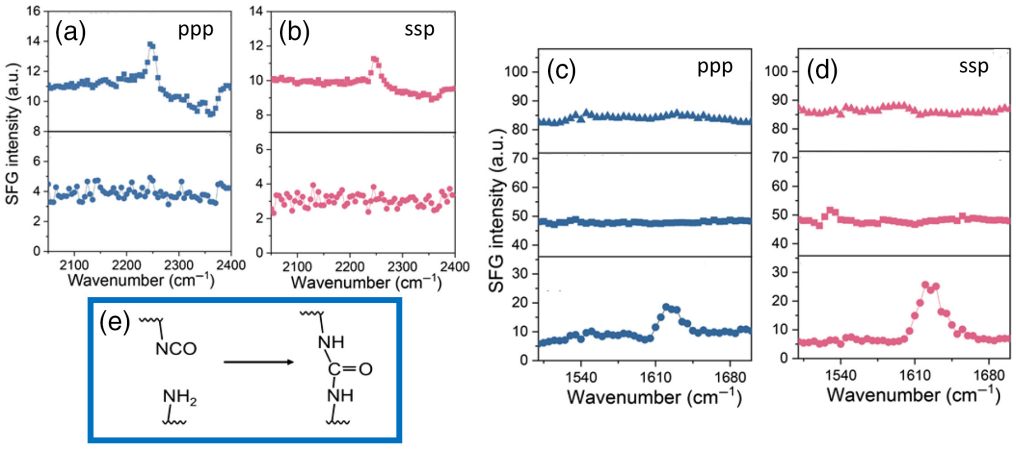

Fig. 10 (a) SFG ppp and (b) ssp spectra collected from the buried primer/PPC interface before (top) and after (bottom) annealing. (c) SFG ppp and (d) ssp spectra collected from the PPC (top), primer (middle) and PPC/primer interfaces (bottom) after annealing. (e) Postulated chemical reaction between isocyanate and amine groups. Adapted from Ref. 64. Copyright 2020, American Chemical Society.

reaction [Figs. 10(c) and 10(d)]. In this study, again SFG detected changes in both the reactant and product of the interfacial chemical reaction as shown in Fig. 10(e), elucidating the molecular mechanism of adhesion between primer and PCC at a buried solid/solid interface.[64]

SFG has been applied to observe chemical reactions of many different systems at buried interfaces. For example, SFG was used to successfully elucidate the adhesion mechanisms of silicone adhesives to various substrates, demonstrating the significance of interfacial aggregation, ordering, and chemical reaction of adhesion promoters used in the silicone adhesives.[26,30,65,66]

3.5 *Molecular Structures of Buried Interfaces in Multi-layered Device*

One challenge of using SFG to examine buried solid/solid interfaces is that SFG can only probe a buried solid/solid interface accessible by the two input beams of the SFG experiment. For the above presented SFG studies, one of the solid media is thin so the input beams can penetrate the thin layer to reach the buried interface. For a multilayered "thick" device, it may not be feasible for the two input beams to reach a specific interface for study. This poses a problem to study buried interfaces using SFG, especially for devices with 3D technology where many buried interfaces exist. To overcome this difficulty, we developed a "milling down" approach which can be used to probe molecular structures or interactions at buried solid/solid interfaces of a multilayered thick device.[67]

Figure 11(a) shows a flip-chip-on-leadframe (FCOL) device. We aimed to probe the buried PI/mold compound interface and the buried mold compound/leadframe interface. Neither interface can be accessed with the input beams of SFG experiments because the light beams cannot penetrate the silicon (top) layer or the leadframe (Cu, bottom). We milled down the device to remove the silicon and part of the PI layer to expose about 1 μm thick PI layer to air [Fig. 11(b)]. Both input beams could then penetrate the thin PI layer to reach the buried PI/mold compound interface. SFG spectra were successfully collected with a prism sample geometry and a window sample geometry (Fig. 12). With the prism geometry, SFG signal can only be collected from the PI surface in the air. The SFG signal detected with the window geometry was contributed by both the PI/air and PI/mold compound interface. Using both SFG spectra, SFG signals contributed from the buried PI/mold compound interface could be deduced to elucidate the molecular structure at this interface. It is worth mentioning that various methods can be used to separate SFG signal contributions from the surface and buried interface of a thin film coating. Examples of

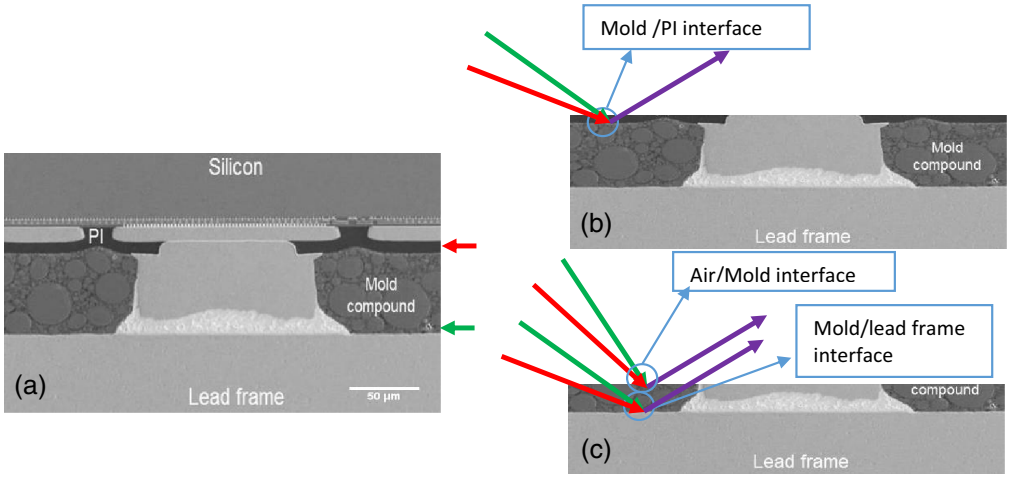

Fig. 11 (a) SEM image of a FCOL device. The red and green arrows are pointing to the PI/mold compound and mold compound/leadframe interfaces respectively. (b) By milling down just the Si chip and some of the PI, the PI/mold compound interface can be analyzed. (c) By further milling through the mold compound, the mold compound/leadframe interface can be probed. It is worth noting that (b) and (c) are not the SEM images of the milled down samples. They are just the schematics obtained by modifying the image shown in (a). Adapted from Ref. 67. Copyright 2018 IEEE.

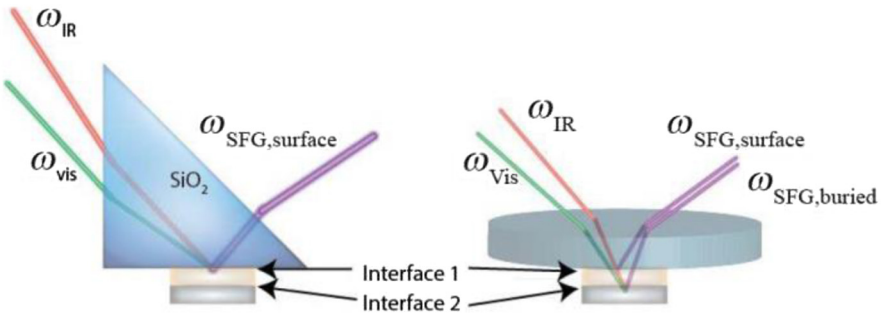

Fig. 12 SFG prism sample geometry (left) and window sample geometry (right) used to collected SFG spectra. Adapted from Ref. 67. Copyright 2018 IEEE.

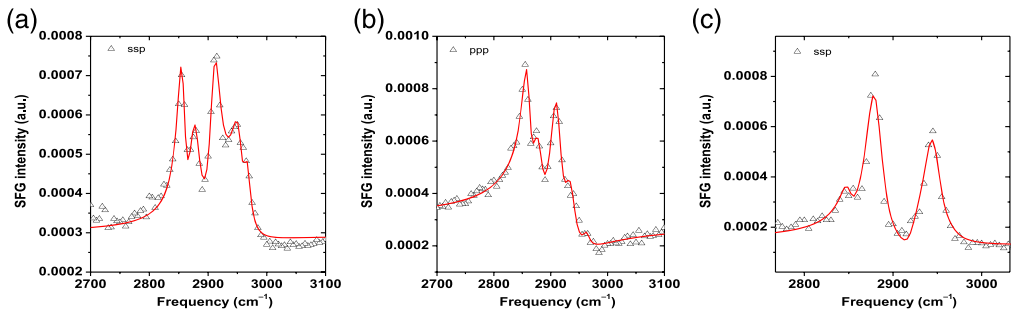

Fig. 13 (a) SFG ssp prism; (b) ppp prism; and (c) ssp window spectra collected from the mold compound layer on lead frame. The dots are experimental data. The lines are fitting results. Adapted from Ref. 67. Copyright 2018 IEEE.

such methods include the SFG studies on films with varied thicknesses[43,50,51] or SFG data collected with different input angles of the laser beams (e.g., by rotating the sample).[45] For the milling down samples studied using SFG here, the method adopted above by collecting SFG spectra with the window and prism is easier for data analysis. The milling down method unlikely altered the buried interface, thus we could use this method to study buried solid/solid interfaces in multilayered thick devices *in situ* nondestructively. Further details about the milling down method will be systematically investigated in the future.

With a similar approach, we continued to mill down the device to expose about 1-μm thick mold compound to air [Fig. 11(c)]. With this sample, SFG spectra were collected using the prism and window geometries to study the buried mold compound/leadframe interface *in situ* nondestructively (Fig. 13). With the SFG spectra shown in Figs. 13(a) and 13(b), which were only contributed by the mold compound/air surface, we could deduce the structure of this surface.[67] The SFG spectrum shown in Fig. 13(c) has signal contributions from both the surface and the mold compound/lead frame interface. With the help of the known spectral parameters of the surface, we could fit this spectrum to obtain the signal contribution from the buried interface to deduce the buried mold compound/lead frame interface structure.[67] It is worth mentioning that this milling down approach is generally applicable, demonstrating the feasibility to probe buried solid/solid interfaces in multilayered thick devices, which is extremely important for studies on devices based on 3D technology.

4 Conclusion

With the rapid development of 3D integration technology including advanced EUV lithography, more and more buried solid/solid interfaces are involved in modern microelectronic devices. It is extremely important to probe such buried interfaces *in situ* nondestructively to understand the molecular structures and molecular interactions at these interfaces. However, it is difficult to characterize such interfaces due to the lack of appropriate metrology which can directly study the buried solid/solid interface *in situ*.

SFG is an excellent metrology, which can provide molecular-level information of buried solid/solid interfaces *in situ* nondestructively, without the need to break the buried interface for study. It is necessary to clarify that here the nondestructive method means that SFG does not require to destruct the buried interface to break the interface for study. Some sample preparation procedures (e.g., milling down) may be required for SFG experiment to study buried interfaces. Such sample preparation procedures may have destructive effect on the sample, but do not destruct the interface we plan to study. In this article, we summarized our recent progress in applying SFG to characterize buried interfaces. We demonstrated that SFG could be applied to study buried interfaces between the porous low-k coating and silicon substrate, showing that plasma treatment, ISE treatment, and silylation repair did not change the buried interface. SFG results on the buried plasma treated polymer/epoxy interface indicated that interfacial structure could be altered by plasma treatment on the polymer surface, leading to lower interfacial methyl coverage and ordering, enhancing adhesion. SFG was also applied to investigate the effect of flux treatment of Cu on the interfacial structure between Cu and epoxy, showing that flux treatment generated a disordered buried interface to improve adhesion. Using SFG, we successfully revealed chemical reaction mechanisms at various buried interfaces *in situ*. With the generally applicable milling down approach, we demonstrated the feasibility to study buried solid/solid interfaces in multilayered thick devices using SFG.

It is worth mentioning that up to date, SFG has not been applied to study many important buried interfaces of devices developed with 3D integration technology including EUV lithography. However, with the progress made in applying SFG to study buried interfaces, we believe that SFG is a unique and powerful metrology to study interfaces important to 3D technology, either with studies on model systems or real products.

Acknowledgment

This research is supported by the University of Michigan. The authors declare no conflicts of interest.

Code, Data, and Materials Availability

This is a review article. All the data were published previously and the original publications were cited in the paper.

References

1. J. Kwon et al., "Three-dimensional monolithic integration in flexible printed organic transistors," *Nat. Commun.* **10**(1), 54 (2019).
2. A. W. Topol et al., "Three-dimensional integrated circuits," *IBM J. Res. Dev.* **50**(4.5), 491–506 (2006).
3. D. Zhang and J. J.-Q. Lu, "3D integration technologies: an overview," in *Materials for Advanced Packaging*, D. Lu and C. Wong, Eds., pp. 1–26, Springer International Publishing, Cham (2017).
4. J. P. Gambino, S. A. Adderly, and J. U. Knickerbocker, "An overview of through-silicon-via technology and manufacturing challenges," *Microelectron. Eng.* **135**, 73–106 (2015).
5. T. Kim et al., "Progress, challenges, and opportunities in oxide semiconductor devices: a key building block for applications ranging from display backplanes to 3D integrated semiconductor chips," *Adv. Mater.*, e2204663 (2023).
6. S. K. Kim et al., "3D stackable synaptic transistor for 3D integrated artificial neural networks," *ACS Appl. Mater. Interfaces* **12**(6), 7372–7380 (2020).
7. P. Zhao et al., "Advanced 3D integration technologies in various quantum computing devices," *IEEE Open J. Nanotechnol.* **2**, 101–110 (2021).
8. G. Yeap et al., "5 nm CMOS production technology platform featuring full-fledged EUV, and high mobility channel FinFETs with densest 0.021 μm^2 SRAM cells for mobile SoC and high performance computing applications," in *IEEE Int. Electron Devices Meeting (IEDM)*, IEEE (2019).

9. E. S. Jung, "4th industrial revolution and boundry: challenges and opportunities," in *IEEE Int. Electron Devices Meeting (IEDM)*, IEEE (2018).
10. B. Sell et al., "Intel 4 CMOS technology featuring advanced FinFET transistors optimized for high density and high-performance computing," in *IEEE Symp. VLSI Technol. and Circuits (VLSI Technol. and Circuits)*, IEEE (2022).
11. Y. R. Shen, "Basic theory of surface sum-frequency generation," *J. Phys. Chem. C Nanomater. Interfaces* **116**(29), 15505–15509 (2012).
12. Z. Chen, Y. R. Shen, and G. A. Somorjai, "Studies of polymer surfaces by sum frequency generation vibrational spectroscopy," *Annu. Rev. Phys. Chem.* **53**(1), 437–465 (2002).
13. X. Lu et al., "Studying polymer surfaces and interfaces with sum frequency generation vibrational spectroscopy," *Anal. Chem.* **89**(1), 466–489 (2017).
14. Y. Fang et al., "Probing surface and interfacial molecular structures of a rubbery adhesion promoter using sum frequency generation vibrational spectroscopy," *Surf. Sci.* **615**, 26–32 (2013).
15. T. Yu et al., "Transport and organization of cholesterol in a planar solid-supported lipid bilayer depend on the phospholipid flip-flop rate," *Langmuir* **32**(44), 11681–11689 (2016).
16. J. Tan et al., "Misfolding of a human islet amyloid polypeptide at the lipid membrane populates through β-sheet conformers without involving α-helical intermediates," *J. Am. Chem. Soc.* **141**(5), 1941–1948 (2019).
17. S. Yamamoto et al., "Molecular events for an epoxy–amine system at a copper interface," *ACS Appl. Polym. Mater.* **2**(4), 1474–1481 (2020).
18. M. Aoki et al., "Segregation of an amine component in a model epoxy resin at a copper interface," *Polym. J.* **51**(3), 359–363 (2019).
19. S. Sugimoto et al., "Reorientation kinetics of local conformation of polyisoprene at substrate interface," *ACS Macro Lett.* **7**(1), 85–89 (2018).
20. M. Inutsuka et al., "Adhesion control of elastomer sheet on the basis of interfacial segregation of hyperbranched polymer," *ACS Macro Lett.* **8**(3), 267–271 (2019).
21. Y. Hong et al., "Concentration-dominated orientation of phenyl groups at the polystyrene/graphene interface," *ACS Macro Lett.* **9**(6), 889–894 (2020).
22. B. Zuo et al., "Effect of local chain conformation in adsorbed nanolayers on confined polymer molecular mobility," *Phys. Rev. Lett.* **122**(21), 217801 (2019).
23. D. H. Gracias et al., "Molecular characterization of polymer and polymer blend surfaces. Combined sum frequency generation surface vibrational spectroscopy and scanning force microscopy studies," *Acc. Chem. Res.* **32**(11), 930–940 (1999).
24. H. Ye et al., "Probing organic field effect transistors *in situ* during operation using SFG," *J. Am. Chem. Soc.* **128**(20), 6528–6529 (2006).
25. C. Zhang et al., "Quantitative molecular level understanding of ethoxysilane at poly(dimethylsiloxane)/polymer interfaces," *Langmuir* **29**(2), 610–619 (2013).
26. C. Zhang et al., "Headgroup effect on silane structures at buried polymer/silane and polymer/polymer interfaces and their relations to adhesion," *Langmuir* **28**(14), 6052–6059 (2012).
27. W. Guo et al., "Probing molecular interactions between surface-immobilized antimicrobial peptides and lipopolysaccharides *in situ*," *Langmuir* **36**(41), 12383–12393 (2020).
28. J. S. Andre et al., "Molecular interactions between amino silane adhesion promoter and acrylic polymer adhesive at buried silica interfaces," *Langmuir* **38**(19), 6180–6190 (2022).
29. Z. Chen, "Surface hydration and antifouling activity of zwitterionic polymers," *Langmuir* **38**(15), 4483–4489 (2022).
30. T. Lin et al., "Probing covalent interactions at a silicone adhesive/nylon interface," *Langmuir* **38**(8), 2590–2600 (2022).
31. J. Wang et al., "Investigating thin silicone oil films using four-wave mixing spectroscopy and sum frequency generation vibrational spectroscopy," *Langmuir* **37**(49), 14540–14549 (2021).
32. S. Zhang et al., "Investigation of the atmospheric moisture effect on the molecular behavior of an isocyanate-based primer surface," *Langmuir* **37**(43), 12705–12713 (2021).
33. L. Shi et al., "Effect of surfactant concentration and hydrophobicity on the ordering of water at a silica surface," *Langmuir* **37**(36), 10806–10817 (2021).

34. N. W. Ulrich et al., "Nondestructive analysis of buried interfacial behaviors of flux residue and their impact on interfacial mechanical property," *IEEE Trans. Compon. Packaging Manuf. Technol.* **8**(6), 982–990 (2018).
35. N. W. Ulrich et al., "Plasma treatment effect on polymer buried interfacial structure and property," *Phys. Chem. Chem. Phys.* **19**(19), 12144–12155 (2017).
36. X. Zou et al., "Investigating the effect of two-point surface attachment on enzyme stability and activity," *J. Am. Chem. Soc.* **140**(48), 16560–16569 (2018).
37. M. Xiao et al., "Molecular interactions between single layered MoS_2 and biological molecules," *Chem. Sci.* **9**(7), 1769–1773 (2018).
38. Z. Chen, "Understanding surfaces and buried interfaces of polymer materials at the molecular level using sum frequency generation vibrational spectroscopy," *Polym. Int.* **56**(5), 577–587 (2007).
39. Z. Chen, "Investigating buried polymer interfaces using sum frequency generation vibrational spectroscopy," *Prog. Polym. Sci.* **35**(11), 1376–1402 (2010).
40. J. M. Hankett et al., "Molecular level studies of polymer behaviors at the water interface using sum frequency generation vibrational spectroscopy," *J. Polym. Sci. B Polym. Phys.* **51**(5), 311–328 (2013).
41. J. N. Myers and Z. Chen, "Polymer molecular behaviors at buried polymer/metal and polymer/polymer interfaces and their relations to adhesion in packaging," *The Journal of Adhesion* **93**(13), 1081–1103 (2017).
42. X. Zhang et al., "*In situ* observation of water behavior at the surface and buried interface of a low-*k* dielectric film," *ACS Appl. Mater. Interfaces* **6**(21), 18951–18961 (2014).
43. J. N. Myers et al., "Nondestructive *in situ* characterization of molecular structures at the surface and buried interface of silicon-supported low-*k* dielectric films," *J. Phys. Chem. B* **119**(4), 1736–1746 (2015).
44. X. Zhang et al., "Probing the molecular structures of plasma-damaged and surface-repaired low-*k* dielectrics," *Phys. Chem. Chem. Phys.* **17**(39), 26130–26139 (2015).
45. J. N. Myers et al., "Plasma treatment effects on molecular structures at dense and porous low-k SiCOH film surfaces and buried interfaces," *J. Phys. Chem. C Nanomater. Interfaces* **119**(39), 22514–22525 (2015).
46. X. Zhang et al., "SFG analysis of the molecular structures at the surfaces and buried interfaces of PECVD ultralow-dielectric constant pSiCOH," *J. Appl. Phys.* **119**(8), 084101 (2016).
47. J. N. Myers et al., "SFG analysis of the molecular structures at the surfaces and buried interfaces of PECVD ultralow-dielectric constant pSiCOH: reactive ion etching and dielectric recovery," *Appl. Phys. Lett.* **110**(18), 182902 (2017).
48. A. Grill et al., "Progress in the development and understanding of advanced low *k* and ultralow *k* dielectrics for very large-scale integrated interconnects—state of the art," *Appl. Phys. Rev.* **1**(1), 011306 (2014).
49. M. Green and M. Maex, *Series in Materials for Electronic and Optoelectronic Applications*, John Wiley & Sons, Chichester, England; Hoboken, NJ (2007).
50. X. Lu et al., "Probing molecular structures of polymer/metal interfaces by sum frequency generation vibrational spectroscopy," *Macromolecules* **41** (22), 8770–8777 (2008).
51. M. Xiao et al., "Effect of interfacial molecular orientation on power conversion efficiency of perovskite solar cells," *J. Am. Chem. Soc.* **139** (9), 3378–3386 (2017).
52. S. Luo and C. P. Wong, "Influence of temperature and humidity on adhesion of underfills for flip chip packaging," *IEEE Trans. Compon. Packag. Technol.* **28**(1), 88–94 (2005).
53. S. Luo and C. P. Wong, "Effect of UV/ozone treatment on surface tension and adhesion in electronic packaging," *IEEE Trans. Compon. Packag. Technol.* **24**(1), 43–49 (2001).
54. P. Hoontrakul, L. H. Sperling, and R. A. Pearson, "Understanding the strength of epoxy-polyimide interfaces for flip-chip packages," *IEEE Trans. Device Mater. Reliab.* **3**(4), 159–166 (2003).
55. N. W. Ulrich et al., "Distinct molecular structures of edge and middle positions of plasma treated covered polymer film surfaces relevant in the microelectronics industry," *IEEE Trans. Compon. Packag. Manuf. Technol.* **7**(8), 1377–1390 (2017).
56. C. Zhang, J. Hankett, and Z. Chen, "Molecular level understanding of adhesion mechanisms at the epoxy/polymer interfaces," *ACS Appl. Mater. Interfaces* **4**(7), 3730–3737 (2012).

57. J. N. Myers et al., "Hygrothermal aging effects on buried molecular structures at epoxy interfaces," *Langmuir* **30**(1), 165–171 (2014).
58. N. W. Ulrich, J. N. Myers, and Z. Chen, "Characterization of polymer/epoxy buried interfaces with silane adhesion promoters before and after hygrothermal aging for the elucidation of molecular level details relevant to adhesion," *RSC Adv.* **5**(128), 105622–105631 (2015).
59. C.-L. Chung, K.-S. Moon, and C. P. Wong, "Influence of flux on wetting behavior of lead-free solder balls during the infrared-reflow process," *J. Electron. Mater.* **34**(7), 994–1001 (2005).
60. B. A. Smith and L. J. Turbini, "Characterizing the weak organic acids used in low solids fluxes," *J. Electron. Mater.* **28**(11), 1299–1306 (1999).
61. J. S. Andre et al., "Interfacial behavior of flux residues and its impact on copper/underfill adhesion in microelectronic packaging," *J. Electron. Packag.* **143**(1), 011004 (2021).
62. B. Li et al., "Observing a chemical reaction at a buried solid/solid interface *in situ*," *Anal. Chem.* **92**(20), 14145–14152 (2020).
63. J. S. Andre et al., "Interfacial reaction of a maleic anhydride grafted polyolefin with ethylene vinyl alcohol copolymer at the buried solid/solid interface," *Polymer* **212**, 123141 (2021).
64. S. Zhang et al., "Nondestructive *in situ* detection of chemical reactions at the buried interface between polyurethane and isocyanate-based primer," *Macromolecules* **53**(22), 10189–10197 (2020).
65. T. Lin et al., "Molecular insights into adhesion at a buried silica-filled silicone/polyethylene terephthalate interface," *Langmuir* **36**(49), 15128–15140 (2020).
66. A. V. Vázquez et al., "Molecular structures of the buried interfaces between silicone elastomer and silane adhesion promoters probed by sum frequency generation vibrational spectroscopy and molecular dynamics simulations," *ACS Appl. Mater. Interfaces* **2**(1), 96–103 (2010).
67. N. W. Ulrich et al., "Probing molecular structures of buried interfaces in thick multilayered microelectronic packages," *IEEE Trans. Compon. Packag. Manuf. Technol.* **8**(7), 1213–1224 (2018).

Shuqing Zhang received her BE degree from Sichuan University in 2017 and her MS degree in the macromolecular science and engineering program at the University of Michigan in 2019. She is currently conducting her PhD studies in the same program at the University of Michigan advised by Prof. Zhan Chen. Her research focuses on understanding the structure-property relationships related to the adhesion and degradation mechanisms of polymer-based materials using analytical techniques.

Guangyao Wu received his BS degree from Nankai University. He is a graduate student in the Department of Chemistry at the University of Michigan, he doing his PhD thesis research advised by Prof. Zhan Chen. He is studying molecular interactions at polymer/solution interfaces to understand anti-icing and antifouling mechanisms of polymer materials. He is also investigating surface structures of coatings under different conditions.

Zhan Chen is Michael D. Morris collegiate professor of chemistry, macromolecular science and engineering, biophysics, and applied physics at the University of Michigan. He received his PhD from the University of California at Berkeley. His current research interests include investigations of molecular structures of polymer interfaces and biological interfaces using nonlinear optical spectroscopic methods. He is also studying degradation mechanisms of polymer materials. He is a senior editor of *Langmuir*.